Supplement of "Parameterizations for global thundercloud corona discharge distributions"

Sergio Soler[1], Francisco J. Gordillo-Vázquez[1], Francisco J. Pérez-Invernón[1], Patrick Jöckel[2], Torsten Neubert[3], Olivier Chanrion[3], Victor Reglero[4], and Nikolai Østgaard[5]

[1]Instituto de Astrofísica de Andalucía (IAA), CSIC, PO Box 3004, 18080 Granada, Spain
[2]Deutsches Zentrum für Luft- und Raumfahrt, Institut für Physik der Atmosphäre, Oberpfaffenhofen, Germany
[3]National Space Institute, Technical University of Denmark (DTU Space), Kongens Lyngby, Denmark
[4]Image Processing Laboratory, University of Valencia, Valencia, Spain
[5]Birkeland Centre for Space Science, Department of Physics and Technology, University of Bergen, Bergen, Norway

Correspondence: F. J. Gordillo-Vázquez (vazquez@iaa.es)

1 Introduction

Regarding the end of the 21st century climate scenario and its comparison with present day, Figure S6 shows a comparison between predicted global annual average geographical distributions of in-cloud coronas in the present day (panels (b) and (d)) and by the end of the 21st century (panels (a) and (c)) climate scenarios using the C_{F2} and C_{F3} thundercloud corona schemes.

5   We find that, in general, the C_{F2} and C_{F3} corona schemes predict large global annual average occurrence rates for thundercloud coronas by the end of the 21st century when compared to present day simulations leading to 3.5 ± 0.01 events s^{-1} (in agreement with ASIM nighttime observations). In particular, for the end of the 21st century, the C_{F2} and C_{F3} based schemes predict global annual averages of 4.33 and 4.09 events s^{-1}, respectively. The standard deviation of the occurrence rates for thundercloud coronas in present day simulations is 0.01 (0.02 for C_{F4}), so that present day occurrence rates are significantly

10   smaller than end of the 21st century projections (4.33 and 4.09).

     One of the most noticeable features in the predicted RCP6.0 future scenario for the end of the century (for the two corona schemes investigated) is the significant increase of the in-cloud corona occurrence rate in the coast of India and Indonesian regions with respect to model results for present day conditions. In general, the C_{F2} and C_{F3} schemes predict similar rate of coronas in the coast of India and in Indonesia. Interestingly, the predicted larger corona rate for the end of the 21st century

15   comes with a lowering of the in-cloud corona rate in some parts of India and the north of South America, and with a rate of in-cloud corona discharges in the Europe / Africa region that remains almost unchanged. The projected variation of the meteorological parameters that influence the occurrence rate of in-cloud coronas are plotted in Figure S7.
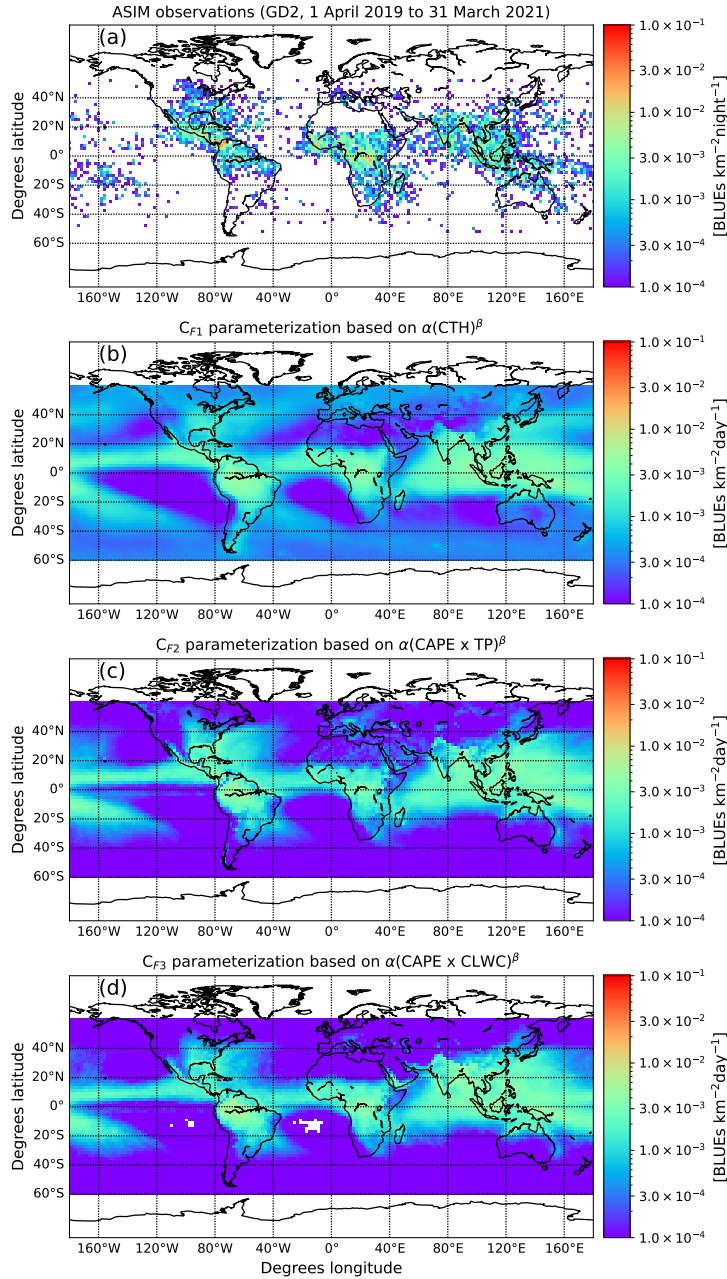
Figure S1. Two-year average (1 April 2019 through 31 March 2021) nighttime geographical distribution of global corona (BLUE) electrical activity in thunderclouds according to the GD-2 distribution derived from ASIM observations (Soler et al., 2022) (a), annual global predictions for BLUE occurrence rate based on CLARA monthly data introduced in the corona (BLUE) parameterizations C_{F1} (b), and ERA5 monthly data introduced in the corona (BLUE) parameterizations C_{F2} (c), and C_{F3} (d).
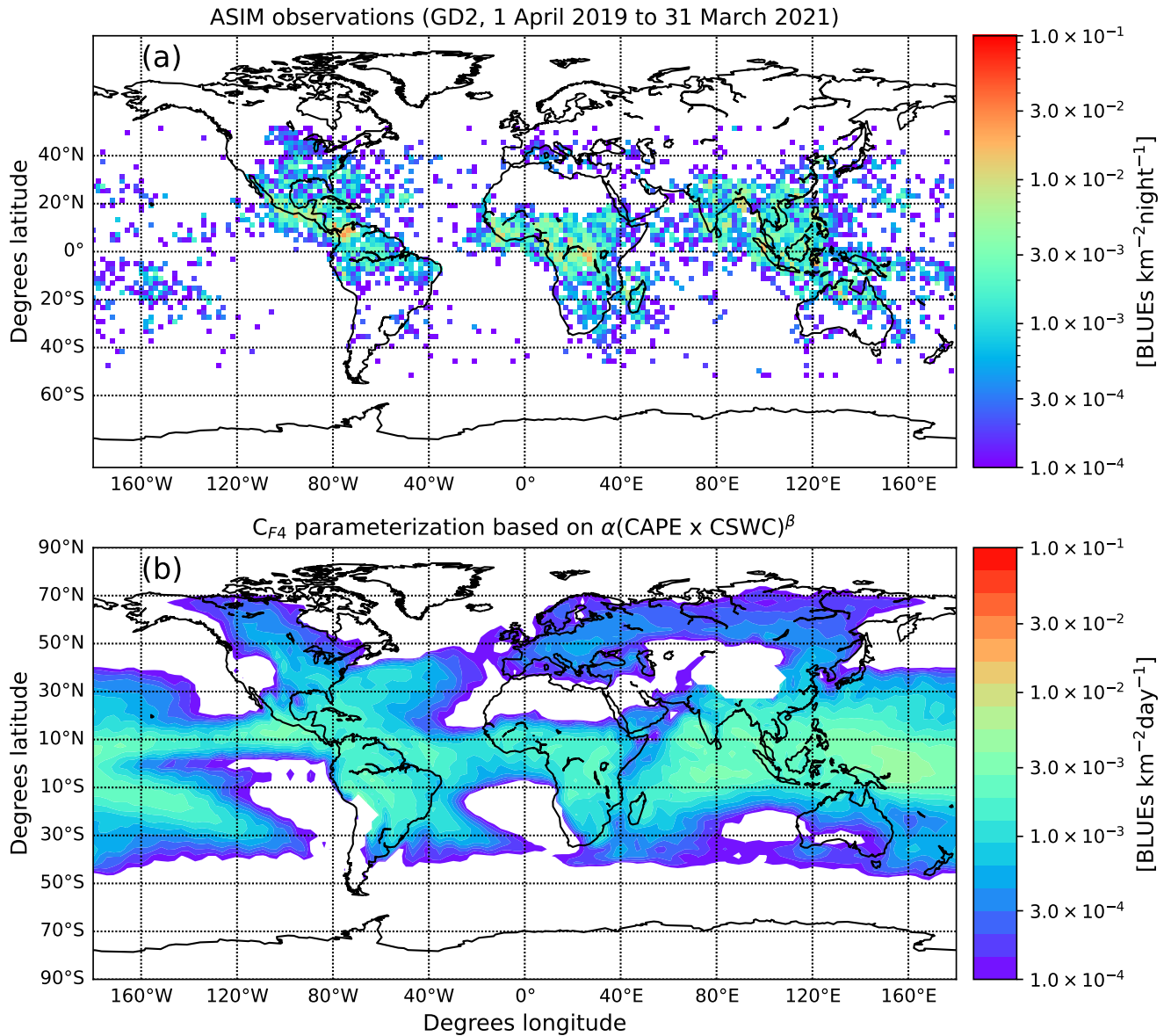
Figure S2. Two-year average (1 April 2019 through 31 March 2021) nighttime climatology of global corona (BLUE) electrical activity in thunderclouds according to GD-2 distribution derived from ASIM observations (a), annual global chemistry-climate model predictions (using 10 year simulations) for BLUE occurrence rate according to the corona parameterization C_{F4} (b). Note that the colorbars have the same scale.
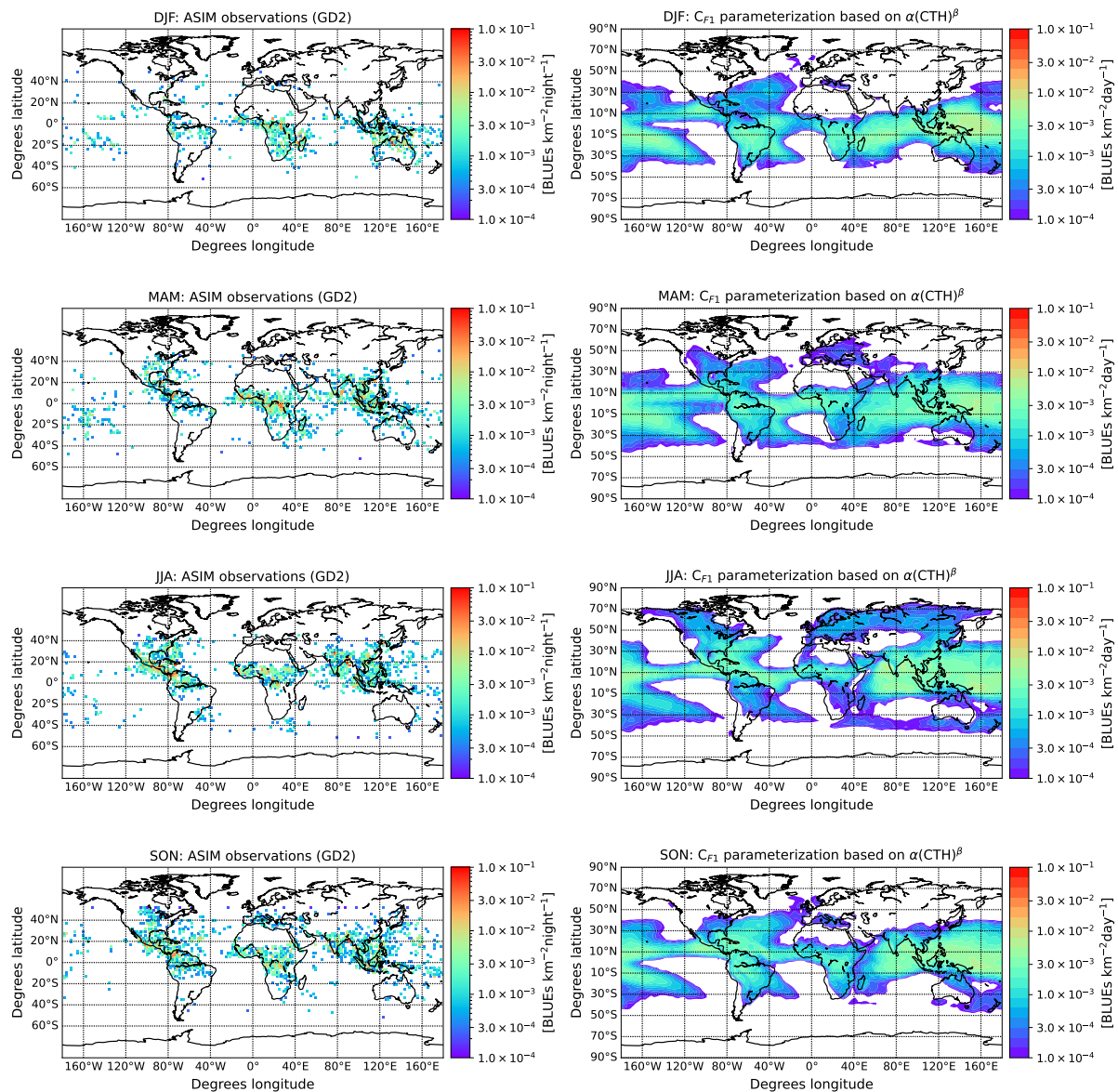
Figure S3. Two-year average (1 April 2019 through 31 March 2021) nighttime seasonal climatology of global corona (BLUE) electrical activity in thunderclouds according to GD-2 distribution derived from ASIM observations resulting in 2.60 (DJF), 3.75 (MAM), 4.01 (JJA) and 3.73 (SON) coronas (or BLUEs) s^{-1} (left column), and global annual average chemistry-climate model predictions (using 10 year simulations) for seasonal BLUE occurrence rate and geographical distribution according to the corona parameterization C_{F1} resulting in 3.38 (DJF), 3.46 (MAM), 3.69 (JJA) and 3.42 (SON) coronas (or BLUEs) s^{-1} (right column). Note that the colorbars have the same scale.
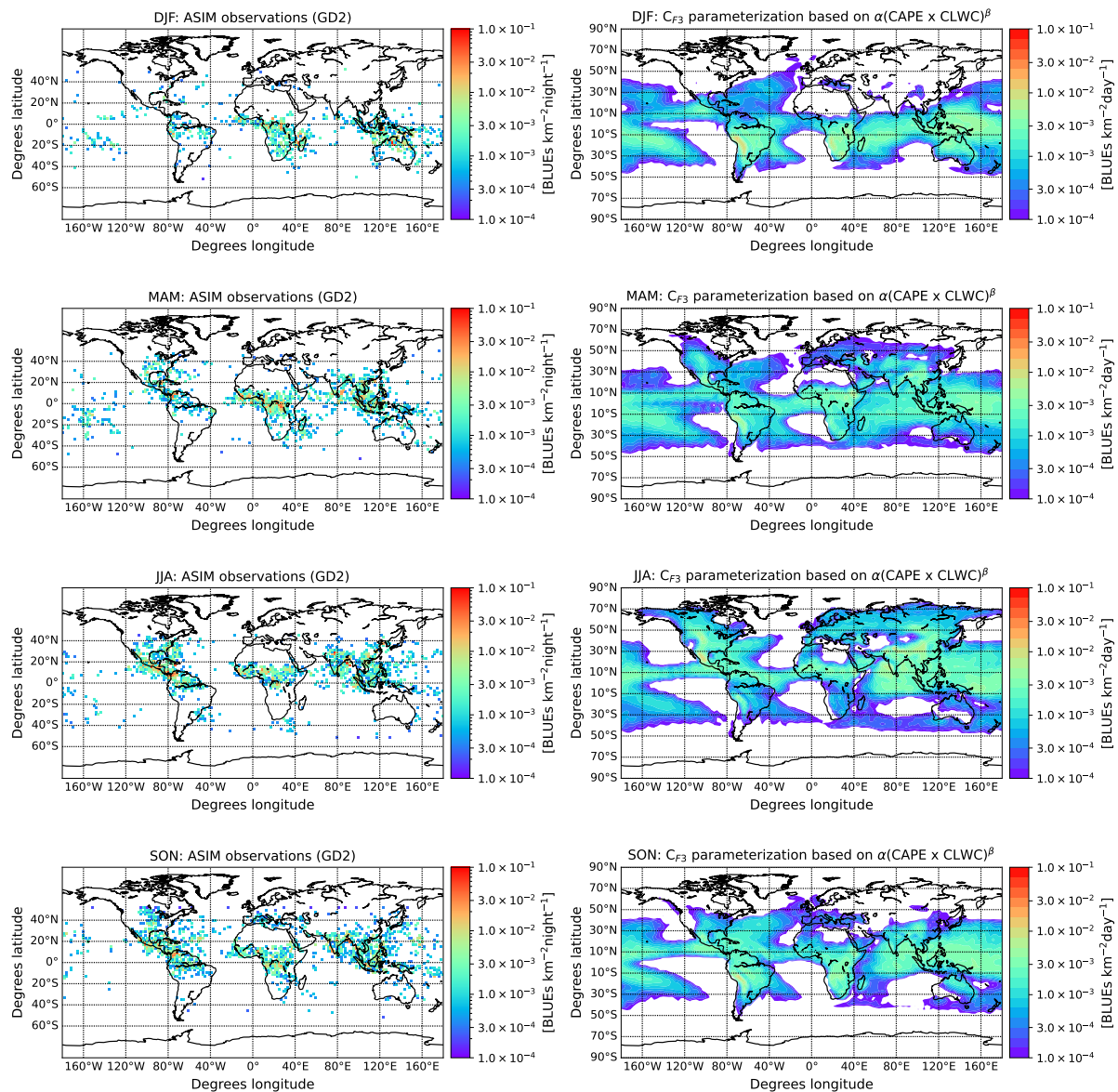
Figure S4. Two-year average (1 April 2019 through 31 March 2021) nighttime seasonal climatology of global corona (BLUE) electrical activity in thunderclouds according to GD-2 distribution derived from ASIM observations resulting in 2.60 (DJF), 3.75 (MAM), 4.01 (JJA) and 3.73 (SON) coronas (or BLUEs) s^{-1} (left column), and global annual average chemistry-climate model predictions (using 10 year simulations) for seasonal BLUE occurrence rate and geographical distribution according to the corona parameterization C_{F3} resulting in 3.23 (DJF), 3.43 (MAM), 3.90 (JJA) and 3.34 (SON) coronas (or BLUEs) s^{-1} (right column). Note that the color-bars have the same scale.
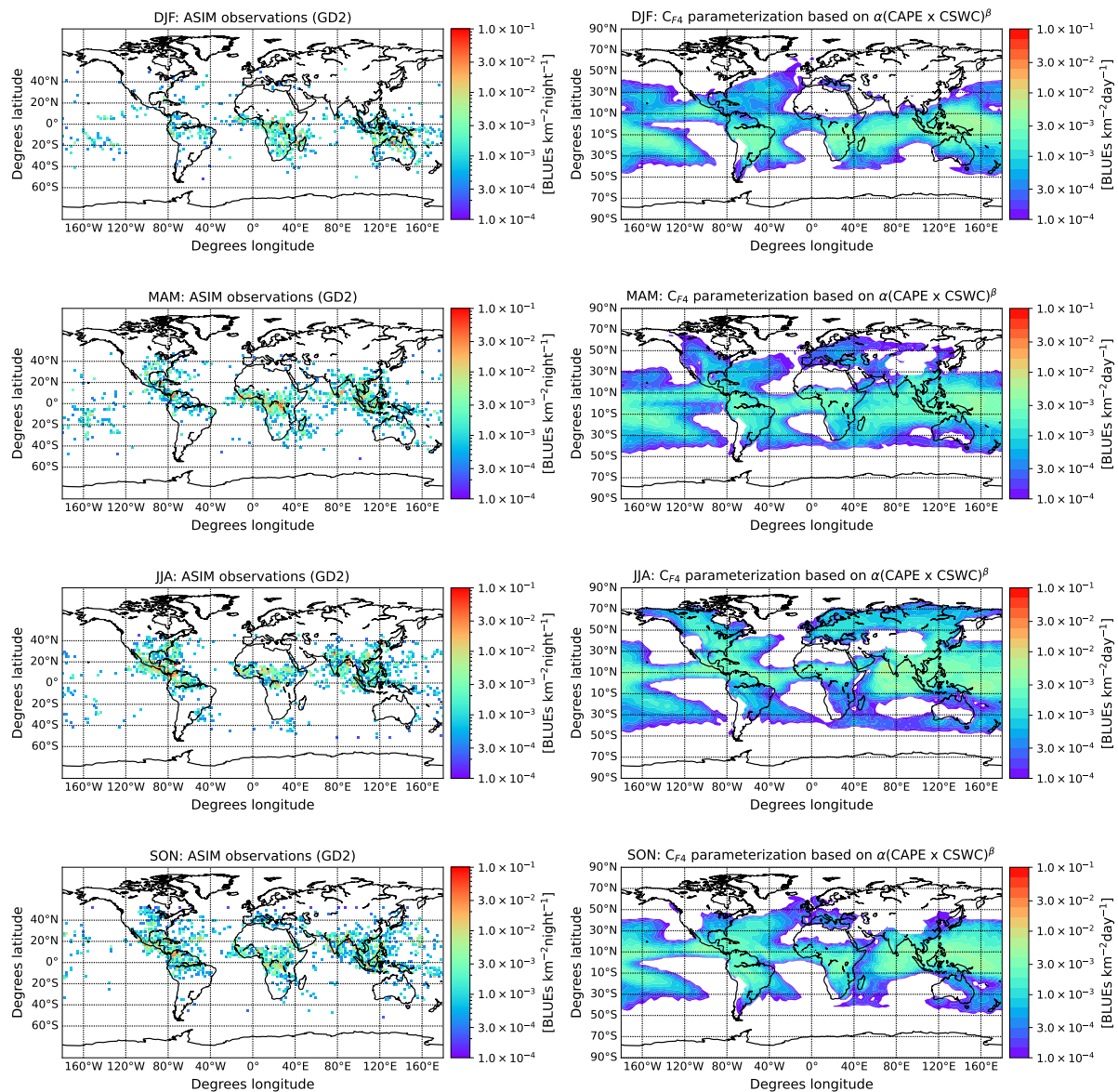
Figure S5. Two-year average (1 April 2019 through 31 March 2021) nighttime seasonal climatology of global corona (BLUE) electrical activity in thunderclouds according to GD-2 distribution derived from ASIM observations resulting in 2.60 (DJF), 3.75 (MAM), 4.01 (JJA) and 3.73 (SON) coronas (or BLUEs) s^{-1} (left column), and global annual average chemistry-climate model predictions (using 10 year simulations) for seasonal BLUE occurrence rate and geographical distribution according to the corona parameterization C_{F4} resulting in 3.32 (DJF), 3.44 (MAM), 3.77 (JJA) and 3.40 (SON) coronas (or BLUEs) s^{-1} (right column). Note that the color-bars have the same scale.
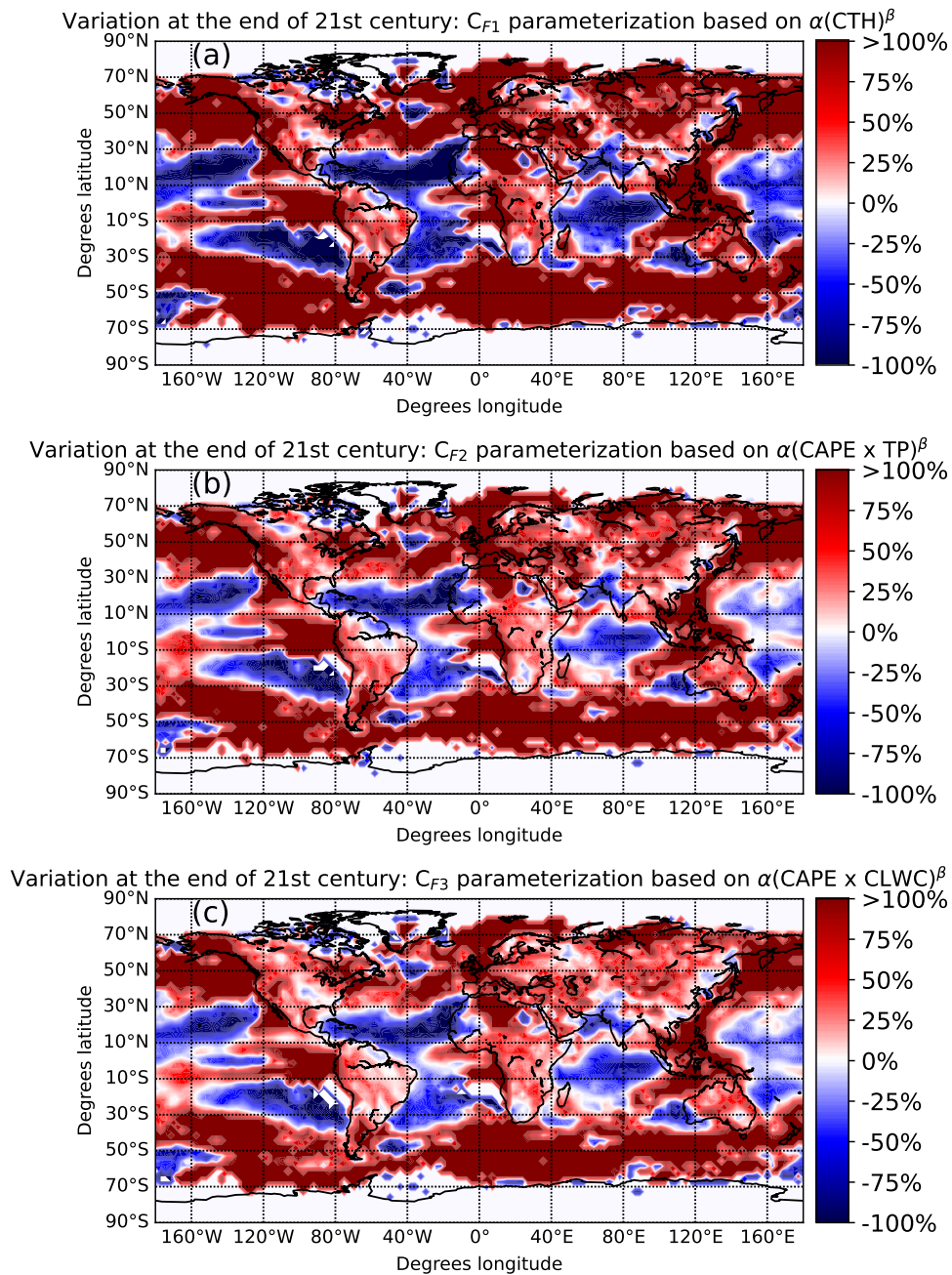
Figure S6. Chemistry-climate simulations showing the variation (percentage) between the geographical distribution for the end of the 21st century and that of present day (global annual average of years 2000 to 2009) of global annual corona (BLUE) occurrence according to different BLUE parameterizations. Panels (a), (b) and (c) correspond to end of 21st century global annual average BLUE occurrence rate of 4.47 coronas s^{-1}, 4.33 coronas s^{-1} and 4.09 coronas s^{-1}, respectively. Note that the color-bars have been deliberately saturated at the upper ends due to the high variability of the plotted risk.
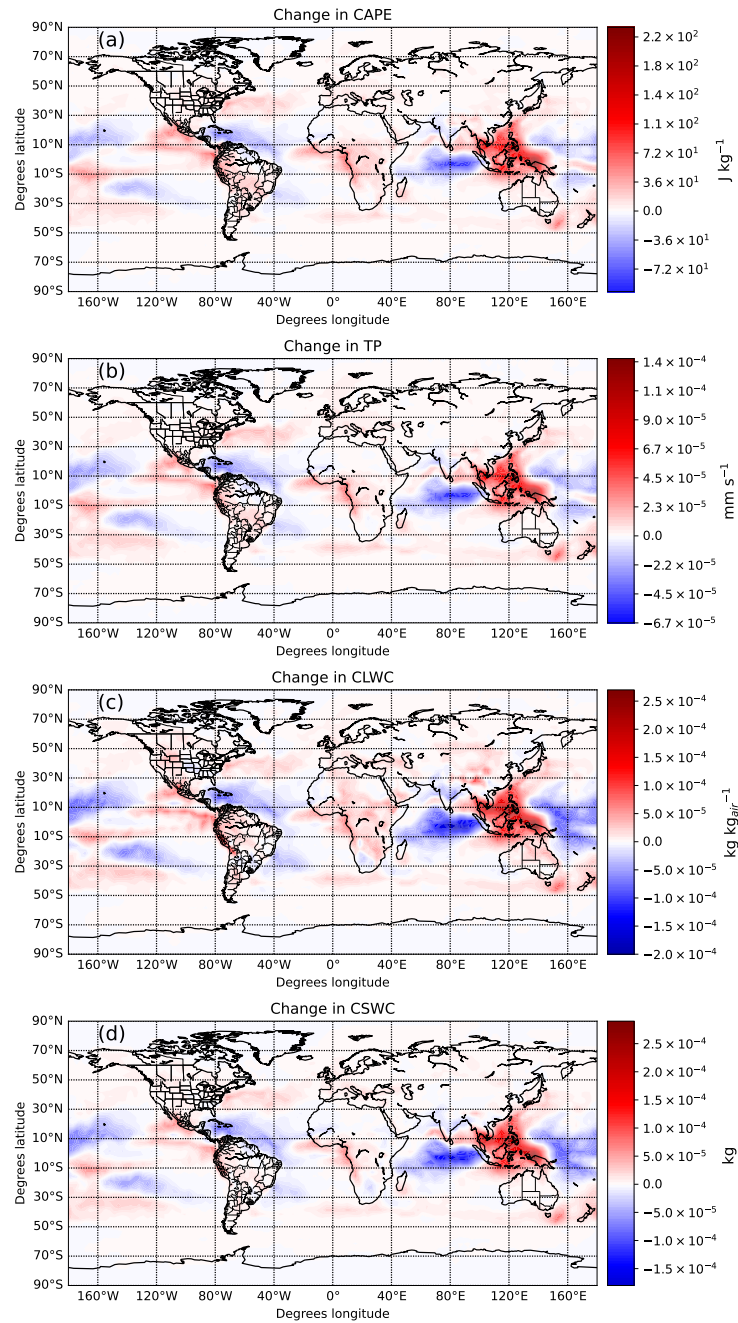
Figure S7. Annually averaged change of CAPE, Total Precipitation (TP), Cloud Liquid Water Content (CLWC) at 450 hPa and Cloud Snow Water Content (CSWC) at 450 hPa. The values are taken only during thunderstorm occurrence. Changes have been calculated between the Representative Concentration Pathway RCP6.0 and present-day simulations.

References

Soler, S., Gordillo-Vázquez, F., Pérez-Invernón, F., Luque, A., Li, D., Neubert, T., Chanrion, O., Reglero, V., Navarro-González, J., and Østgaard, N.: Global distribution of key features of streamer corona discharges in thunderclouds, Journal of Geophysical Research: Atmospheres, p. e2022JD037535, 2022.